ORIGINAL RESEARCH

Enhanced photocatalytic applications of chitosan-encapsulated silver sulfide quantum dots

Article history:
Received: 12-02-2023
Revised: 21-06-2023
Accepted: 01-07-2023

Ambalika Sharma[a], Rahul Sharma[b], Asha Kumari[c]

Abstract: This study explores the synthesis, properties, and applications of chitosan-encapsulated silver sulfide (Ag_2S) quantum dots (QDs) for biological applications. The investigation focuses on the fluctuations in the physico-chemical characteristics of chitosan Ag_2S QDs, which can be carefully studied due to their environmental activity. X-ray diffraction (XRD) measurements reveal that chitosan-coated Ag_2S QDs exhibit higher-intensity peaks. The XRD analysis reports a range of crystallite sizes, with a minimum size of 8 nm and a maximum size of 12 nm. Fourier-transform infrared spectroscopy confirms the presence of chitosan through the detection of functional group peaks. High-resolution transmission electron microscopy studies indicate that the size of the artificial QDs is 6 nm. Energy-dispersive X-ray spectroscopy verifies the composition of chitosan-encapsulated Ag_2S QDs. Moreover, the chitosan Ag_2S QDs demonstrate exceptional photocatalytic activity, as evidenced by the degradation of 92% of methylene blue dye within 1 h. This research provides valuable insights into the synthesis, properties, and potential applications of chitosan-encapsulated Ag_2S QDs in diverse fields.

Keywords: Encapsulation; Silver sulfide (Ag_2S); Quantum dots; HRTEM; XRD; FTIR; EDX.

[a] Department of Chemistry, Career Point University, Hamirpur, Himachal Pradesh 176041, India. Centre for Nano-Science & Technology, CPU, Hamirpur, Himachal Pradesh 176041, India.

[b] Department of Chemistry, Career Point University, Hamirpur, Himachal Pradesh 176041, India. Centre for Nano-Science & Technology, CPU, Hamirpur, Himachal Pradesh 176041, India.

[c] Department of Chemistry, Career Point University, Hamirpur, Himachal Pradesh 176041, India. Centre for Nano-Science & Technology, CPU, Hamirpur, Himachal Pradesh 176041, India.
Corresponding author:
Postal address: Department of Chemistry, Career Point University, Bhoranj (Tikker-kharwarian), Hamirpur, MDR 35, Himachal Pradesh, India, 176041.
Tel.: +918219658940.
asha.che@cpuh.edu.in; ash885124@gmail.com

1. INTRODUCTION

The main strategies to reduce the unfavorable environmental effects of hazardous waste, toxic pollutants, and infection-causing microorganisms are photo-oxidation and microbiological inhibitory capabilities (Abdi-Ali *et al.*, 2014; Andrade *et al.*, 2012;Anitha *et al.*, 2011). Artificial compounds including colors, phenols, and pesticides pollute the effluents from the material, paper, and agricultural industries. These pose a major risk to human health and have a negative impact on the biological system because they are poisonous and cancer-causing in nature.The general public and administrative experts throughout the world are quite concerned about the regularly rising levels of these synthetic compounds in the climate, specifically in water bodies, as they are steadily disintegrating (Anpo *et al.*, 1987). Metallic nanoparticles, in particular silver-based nanoparticles, stand out enough to be observed to increase the interest in their cleansed qualities against various microbes and pollutants. Silver-based chemicals are safe for healthy cells but very toxic for bacteria (Colmenares & Luque, 2014; Sharma *et al.*, 2021). The development of biofilm is triggered by bacterial colonization on hard surfaces, which is a major cause of nosocomial infections. Photocatalysis is a type of complex oxidative process. It relies on the electron-hole pairs that photon absorption

forms in semiconductor materials, which can subsequently cause the system to release free radicals like hydroxyl to redox the chemicals absorbed on the surface of a photocatalyst (Duran *et al.,* 2005; Gemmell *et al.,* 2006; Habiba *et al.,* 2015).The lifetime of these photo-generated charges is being increased by scientists. It has been noted that when using electrons, sacrificial reagents are typically needed to consume holes, and vice versa. Recently, the importance of using both electrons for reduction and holes for carrying out important processes has increased (Kumar *et al.,* 2021). The advantages of polymeric materials, such as their beneficial action over a wide range, their clarity in visible light, and their solubility, make them a good choice. A few specific polymers may form stable suspensions in water and are dispersible. In the literature, there is a simple procedure to create Ag_2S QDs-chitosan nanospheres with S nitrosothiol functional groups. The produced nanospheres, when exposed to UV or visible light, could release NO under physiological settings, and if a NIR light source activated them, they would generate NIR fluorescence (Tan *et al.,* 2013). A straight-forward chemical process to create chitosan, silver nanoparticles, and chitosan-silver nanocomposite. Good antibacterial and anticancer characteristics can be found in the CS-Ag nanocomposite (Govindan *et al.,* 2012). Chemical precipitation was used to create Mn^{2+} and $Fe3^{+-}$ doped ZnS colloidal quantum dots (QDs) that were encapsulated in chitosan. Dopants were used to create chitosan-capped ZnS QDs at various doping doses (Raghuram *et al.,* 2016). A straightforward and repeatable method to generate chitosan (CS)-encapsulated gold-silver nanoflowers by progressively adding chitosan, chloroauric acid, silver nitrate, and ascorbic acid to water at room temperature This is a straightforward and reliable one-pot, seed-free, and surfactant-free synthetic technique (Zhang *et al.,* 2015).

By allowing the photo-catalyst nanoparticles to spread in water and link with color atoms, the polymer shells in this way enable this (Iijima & Kamiya, 2009; Huh & Kwon, 2011). Additionally, it has been found that the movement of the photo-generated electrons is significantly influenced by the nanoparticles' surface-level contact with the polymer (Jose *et al.,* 2018). One of the crucial steps in heterogeneous photocatalysis processes is adsorption. A significant factor impacting photodegradation effectiveness is the adsorption of pollutants on the material's surface. The rate of photocatalytic breakdown may be accelerated by the high adsorption capacity of the photocatalyst (Kusiak-Nejman *et al.,* 2021). Numerous studies have examined the claim that too-broad band gaps in a single semiconductor photocatalytic material result in lower photocatalytic performance. They, therefore, have limited light absorption and poor redox capabilities, which cause photogenerated electron-hole pairs to recombine quickly and reduce their photocatalytic efficacy (Dutta *et al.,* 2023). The polymer's sustainability, bio-restorability, and environmental friendliness not only support the need for a good photocatalyst but also increase the nanocomposite's capacity for adsorption and degradation (Sudhaik *et al.,* 2023). Photo-catalysis is an adventitious technique over other techniques. Biological processes such as precipitation, coagulation, flocculation, ion exchange, membrane filtration, and reverse osmosis are a few examples of water remediation techniques that have been developed for the removal of contaminants, including organic pollutants. Acids, phosphates, hazardous heavy metals, nitrates, colors, etc. There are certain drawbacks to these procedures, such as their low removal effectiveness, cost inefficiency, length of time required, significant creation of sewage sludge, small-scale applicability, and generation of harmful by-products that accumulate in the environment (Hasija *et al.,* 2019). The up-conversion is also impacted by various heteroatoms, doping, and other surface conditions (Sudhaik *et al.,* 2022). The two reaction sites must be kept apart to prevent reverse reactions. Co-catalysts, both metal- and non-metal-based, can be used to boost the number of active sites for photocatalytic reactions as well as trap-free carriers. Although several studies have reported pyro-metallurgical to hydrometallurgical processes to recover metal values from e-waste, the hydrometallurgical route has been noted as the most advantageous because it is more predictable, uses low temperatures, and requires less investment to be implemented. One of the most crucial and difficult tasks is to create a highly efficient and selective metallic leaching method that may result in less complex leaching solutions prepared for post-leaching metal ion recovery. It should be highlighted that even though the leaching processes are an essential part of the metal recovery procedures, the approaches used are largely empirical, and only a small number of papers have examined the processes from a thermodynamic point of view prior to their use. The development of successful processes can be based on the design of these procedures

based on a thermodynamic analysis, which also decreases the amount of resources needed for research —a crucial topic for real-world applications (Barragan *et al.,* 2021).

The novelty of this work is that it successfully encapsulates silver sulfide QDs using chitosan and uses the synthesized samples for environmental applications. By degrading 92% of the harmful methylene blue (ME) dye, which is also harmful to humans and the environment, we have succeeded in achieving our goal. Chitosan is a non-toxic, biodegradable, and biocompatible material that can be used to encapsulate a range of active substances with potential applications. We have also made an effort to look into how the polymer chitosan affects applications like color deterioration by photo-catalysis as well as structural, morphological, and other aspects. The synthesized silver sulfide QDs were characterized using XRD, UV, Fourier-transform infrared (FTIR), High-resolution transmission electron microscopy (HRTEM), and Energy-dispersive X-ray spectroscopy(EDX). Results from the photodegradation of the ME dye in this experiment were quite encouraging (Li *et al.,* 2008).

2. METHOD

2.1. Synthesis of chitosan encapsulated silver sulfide QDs

The creation of chitosan-encapsulated silver sulfide QDs requires two steps. We initially created silver sulfide QDs, and then, in a subsequent phase, chitosan was used to encapsulate the created silver sulfide QDs. Then the collected samples undergo characterization like XRD, HR-TEM, EDX, and FTIR. For crystallite size, XRD is used. HR-TEM is used to calculate the average particle size of synthesized silver sulfide QDs. EDX and FTIR are used for confirmation of composition and functional groups.

2.2. Synthesis of silver sulfide QDs

First, wet chemistry was used to create silver sulfide QDs (Sharma *et al.,* 2023). 1 ml of ethylene glycol was added after 1 g of $AgNO_3$ had been dissolved in distilled water. The mixture is then heated to 65°C while being constantly stirred. After that, ammonia was gradually added while being heated and stirred continuously to achieve a pH of 10. The solution was then gradually supplemented with various volumes of 1% 3-MPA (1, 3, 5, 7, and 9 ml) while being continuously stirred. The solutions were then stirred and heated for 2.5 h under ideal circumstances. The samples were given time to cool after 2.5 h for 4-5 h. The samples that were obtained were dark brown. The samples were then cleaned with distilled water and centrifuged five times at a speed of 2000 rpm. After being collected in a petri dish, the samples were dried for 3days at 50°C until they were no longer dry.

2.3. Formulation of silver sulfide QDs encapsulated chitosan

Then, for the next 5-7 min, at a temperature of 20-30°C, 100 ml of chitosan solution (0.02 g of granules dissolved in 100 ml of 1% (w/v) acetic acid solution) was added to synthesized silver sulfide QDs (El-Khawaga *et al.,* 2020). Samples were placed on a shaker, left to shake for 24 h, and then collected. A sample reduced with 1 ml of 3-MPA is labelled as Chit AG (1). A sample reduced with 3 ml of 3-MPA is labelled as Chit AG (2). A sample reduced with 5 ml of 3-MPA is labelled as Chit AG (3). A sample reduced with 7 ml of 3-MPA is labelled as Chit AG (4). A sample reduced with 9 ml of 3-MPA is labelled as Chit AG (5).

2.4. Instrumentation

In the lab at I.I.T. Ropar, data from an X-ray diffractometer (XRD) were recorded. The vertical theta-theta range was employed to record XRD data in the 2 = 20°-80° range. The rapid solid-state detector-equipped CuK radiation, with K = 1.5418, was employed. In P.U. Chandigarh, researchers employed HR-TEM (model: JEM2100 PLUS Electron Microscope by JEOL Company) to examine the realistic images of the manufactured samples. 200 kV was the HR-scanning TEM's voltage range. To identify the functional groups contained in the synthesized sample at I.I.T. Ropar, Fourier transform infrared (FTIR; model: Perkin Elmer) spectroscopy was performed. To determine the true composition of the synthesized sample at I.I.T. Ropar, EDX was performed.

2.5. Photocatalytic activity

The synthesized samples' photocatalytic activity was assessed. To determine whether manufactured materials had any photocatalytic activity, the degradation of the ME dye was investigated at pH 8-10.

On the synthesized samples exposed to sunlight, a small modification to the previously outlined technique was applied (Orooji *et al.*, 2020). Initially, 10 mg/L dye solutions were made. 100 ml of the dye solution was then added to the beaker. First, dye solutions containing 10 mg/L were created. Following this, 100 ml of dye solution was poured into a beaker, and 5 ml of each sample of Chit AG (1), Chit AG (2), Chit AG (3), Chit AG (4), and Chit AG (5) were added individually and continuously stirred while exposed to sunlight. 5 mL of suspension were collected at regular 15-min intervals throughout the irradiation. Afterwards, to separate the photocatalyst from the solution, the solution was centrifuged at 10,000 rpm for 5 min. Using a UV-visible spectrophotometer, the absorption spectra were then measured to determine if the encapsulated silver sulfide QDs were degrading the dye or not. Equation 1, in which C_o represents the starting dye concentration and Ct represents the dye concentration at various irradiation durations, was used to calculate the percentage of dye degradation.

$$\text{Photocatalytic degradation (\%)} = \frac{C0 - Ct}{C0} \quad \textbf{(1)}$$

3. RESULTS AND DISCUSSIONS

3.1. XRD analysis

The average crystallite size of Chit AG (1), Chit AG (2), Chit AG (3), Chit AG (4), and Chit AG (5) lies in the range of 8-12 nm. The average crystallite size of the synthesized samples decreased with the increased amount of 3-MPA. The obtained crystallite size, d-spacing, strain, and dislocation density of QDs are illustrated in Table 1, given below12 nm is the highest reported crystallite size of the synthesized samples, and 8 nm is the minimum crystallite size of the synthesised samples, as shown in Table 1. Figure 1 represents the XRD peaks of the synthesized samples. Crystallite size is calculated by the Scherrer formula, which is given in equation 2 (Muniz *et al.*, 2016):

$$D = K\lambda / (\beta \cos \theta) \quad \textbf{(2)}$$

The obtained results are in good correlation with the literature (Magesh *et al.*, 2018). Values of h, k, l (miller indices) are according to the literature (Alshehri *et al.*, 2020).

Quantum dots	Crystallitesize (D) nm	d-Spacing(d) nm	Strain	Dislocation density (d) (nm^2)
Chit AG (1)	8	1.549	0.00575	95.26
Chit AG (2)	9	1.895	0.00470	112.73
Chit AG (3)	10	2.255	0.00379	135.99
Chit AG (4)	11	2.498	0.00275	161.20
Chit AG (5)	12	2.698	0.00201	190.12

Table 1. Representing the calculated crystallite size, d-spacing, strain and dislocation density of synthesized samples.

3.2. FTIR spectroscopy analysis

The interaction of silver sulfide QDs encapsulated in chitosan was confirmed by the FTIR spectra. Figure 2 represents the FTIR graphs of Chit AG (1), Chit AG (2), Chit AG (3), Chit AG (4), and Chit AG (5). The FTIR spectra of non-encapsulated silver sulfide QDs vary from those of encapsulated silver sulfide QDs (Sharma *et al.*, 2023) because of the absence of polymer. The obtained results are in good agreement with the literature. The N-H vibration of the chitosan is related to the peak at 1634 cm^{-1}. Additionally, the C-O in the ether group is at 1071 cm^{-1}, while the C-N vibration of the amino group is at 1416 cm_{-1} (Khawaga *et al.*, 2020).

Sulphur and silver are showing peaks at 649 cm^{-1} and 548 cm^{-1}, respectively.

3.3. EDX analysis

The elemental composition of encapsulated silver sulfide QDs encapsulated in chitosan was investigated using EDX characterization. In the spectrum, the peaks of silver (Ag), sulphur (S), carbon (C), nitrogen (N), and oxygen (O). Figure 3 represents the EDX of Chit AG (1), Chit AG (2), Chit AG (3), Chit AG (4), and Chit AG (5).

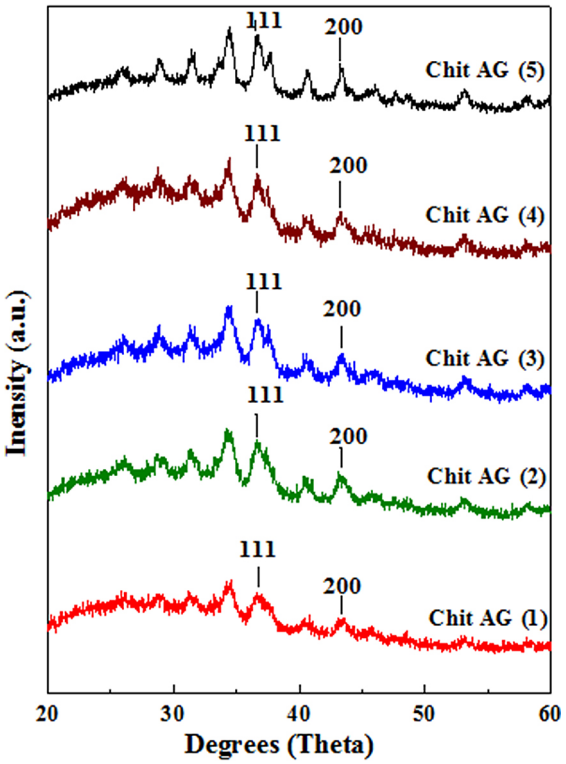

Figure 1. Representing XRD patterns of Chit AG (1), Chit AG (2), Chit AG (3), Chit AG (4), Chit AG (5).

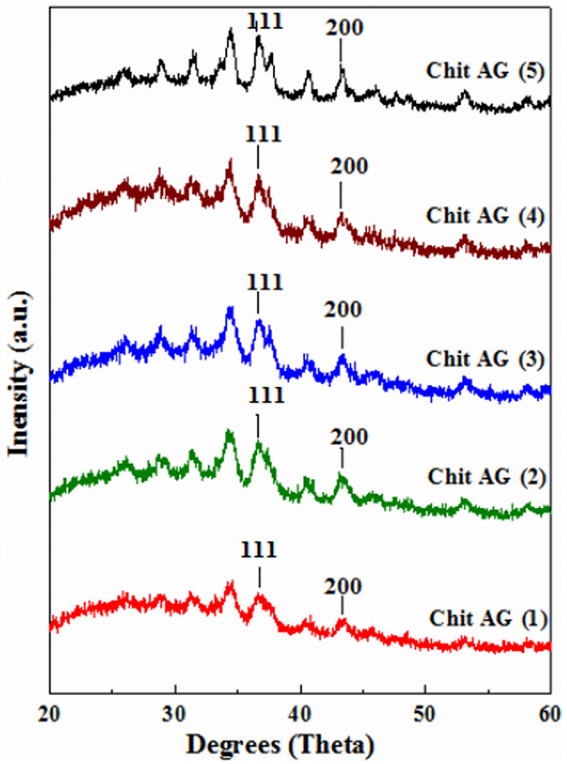

Figure 2. Representing the FTIR graphs of Chit AG (1), Chit AG (2), Chit AG (3), Chit AG (4), Chit AG (5).

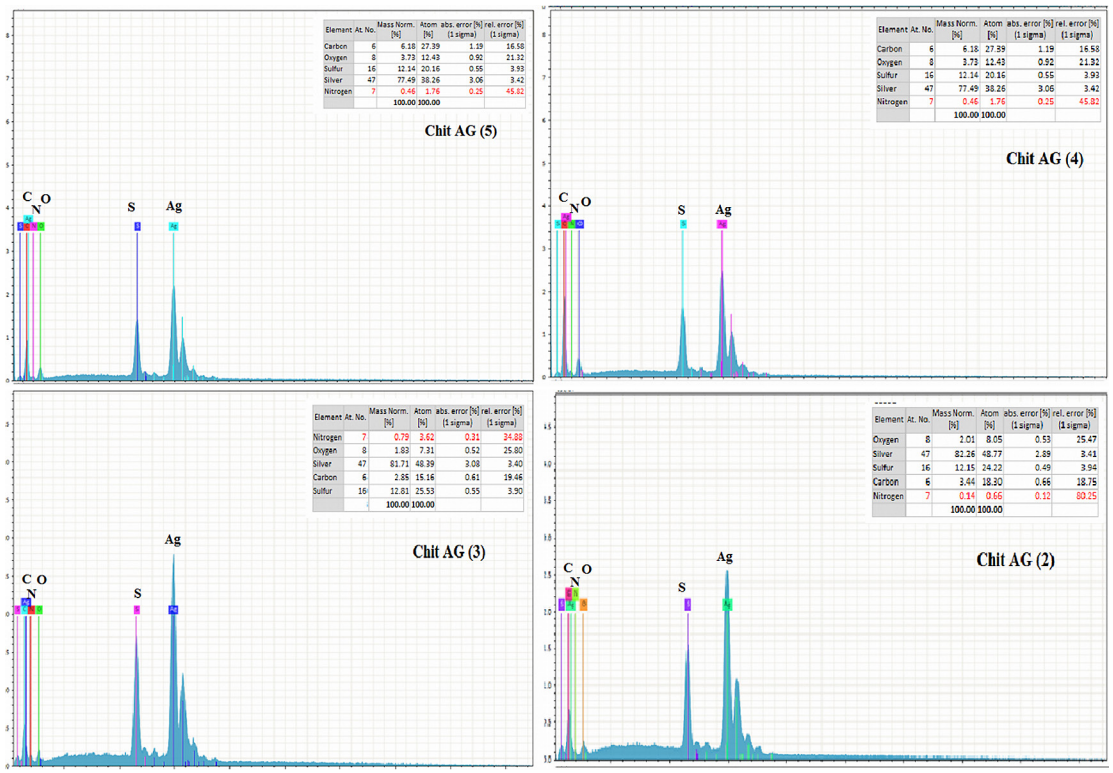

Figure 3a. Representing the EDX of Chit AG (2), Chit AG (3), Chit AG (4), Chit AG (5).

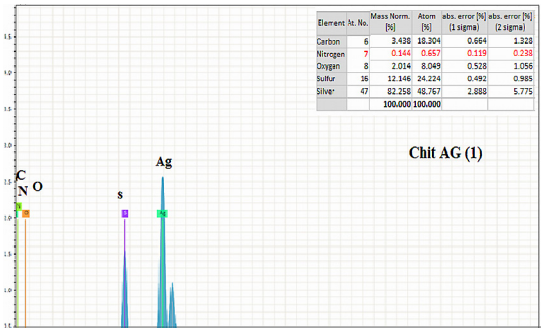

Figure 3b. Representing the EDX of Chit AG (1),

3.4. HR-TEM analysis

Utilising HR-TEM, particle size and shape were studied. The HR-TEM results of the studied particles are depicted in the image, and Image J software is used to determine particle size. The HR-TEM clearly shows that the shape of the particles is spherical, which corresponds to the literature (Manikandan & Sathiyabama, 2015). The average calculated particle size of Chit AG (1) is 6 nm. Figure 4 shows the particles of synthesized samples.

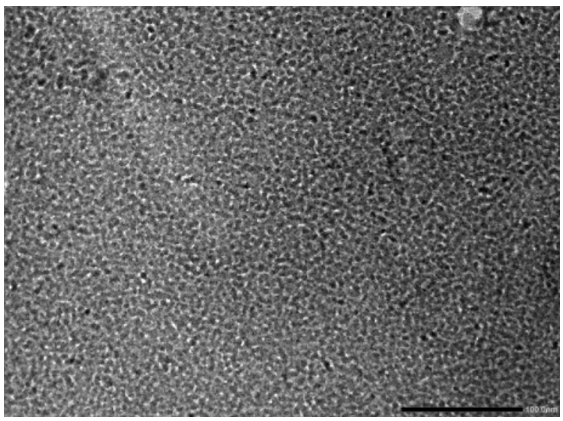

Figure 4. Representing the HRTEM of Chit AG (1).

4. APPLICATION

4.1. Photocatalytic activity

The action was carried out by the sunlight's rays. The degradation of the dye was evaluated using a UV-visible spectrophotometer. ME dye aqueous solution was used as a target pollutant to evaluate the photocatalytic performance of generated chitosan Ag_2S QDs. The ME dye absorbs most fully at a wavelength of 664 nm. To calculate the percentage of dye degradation, the absorbance spectrum's strength of absorption was employed. After 1 h of exposure to sunlight, the degradation efficiencies of Chit AG (1), Chit AG (2), Chit AG (3), Chit AG (4), and Chit AG (5) are 92%, 67.9%, 48%, 29.8%, and 11%, respectively. The obtained results are much better than the literature (Khawaga *et al.*, 2020). 10 mg of photocatalyst from each sample was used separately to degrade the dye sequentially. The highest results of degradation were achieved by Chit AG (1). Photocatalytic degradation is directly proportional to the photocatalyst dose. The information obtained demonstrated that as particle size decreased, degrading efficacy increased (Dodd *et al.*, 2006). With decreasing particle size, QD's recombination of the electron-hole pair is significantly lowered because of its increased surface area-to-volume ratio. The smallest QDs are consequently expected to have stronger photocatalytic activity than their bulk constituents. Electrons and holes are able to participate in the chemical reaction more quickly by hastening their migration to the surface of QDs. Another possibility is that chitosan increases the strength of light absorption and dye degradation (Ma *et al.*, 2020). Figure 5 (A, C) represents the degradation of dye, and (B,D) represents the time-dependent graph of photocatalytic degradation of samples Chit AG (1) and Chit AG (5). Photocatalytic degradation and time-dependent graph of sample Chit AG (2) are in supplementary file S1, photocatalytic degradation and time-dependent graph of sample Chit AG (3) are in supplementary file S2, and photocatalytic degradation and time-dependent graph of sample Chit AG (4) are in supplementary file S3.

4.2. Effect of pH on degradation of ME dye

Due to the effect on the surface charge of the photocatalyst that affects dye degradation, the pH is thought to be the primary parameter in the photocatalytic process. Therefore, an effort was made to research how pH affects the breakdown of ME at pH levels between 8 and 10 (Figure 6), and it was changed before adsorption. We also looked into photocatalytic degradation in a pH 3 acidic environment, where the impact was minimal. We also looked into photocatalytic degradation in a pH 3 acidic environment, where the impact was minimal, so we have not mentioned that in the figure. ~90% of degradation is achieved at pH 10. The reason might be the increase in hydroxyl ions which is boosting adsorption (Vasiljevic *et al.*, 2020).

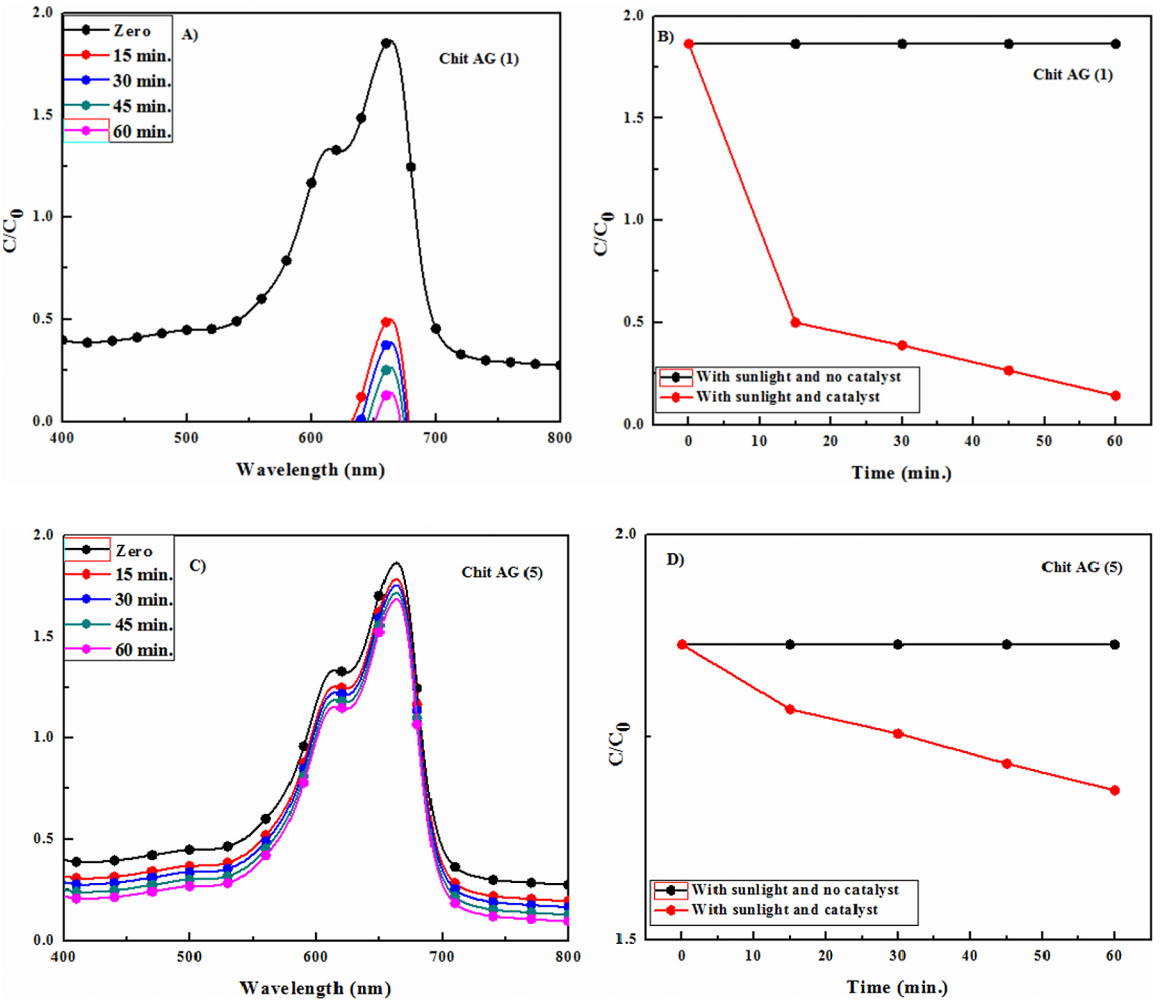

Figure 5. (A,C) representing the degradation of dye and (B,D) representing the time-dependent graph of Photocatalytic degradation of samples Chit AG (1) and Chit AG (5).

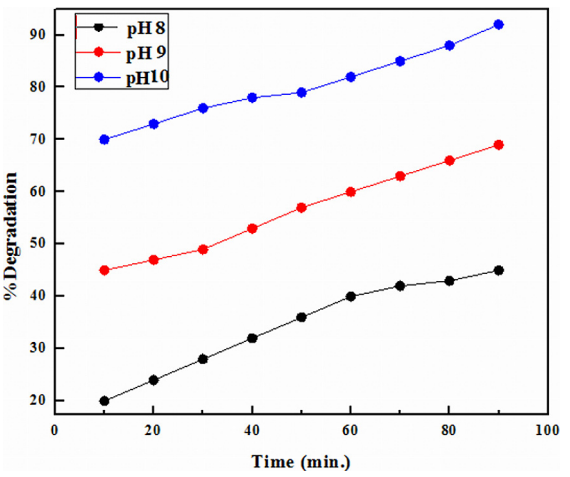

Figure 6. Representing the degradation percentage of methylene blue by Chit AG (1).

4.3. Mechanism of photocatalytic action of degradation of dye

According to certain accounts, radical species created during semiconductor photo-excitation are the cause of dye degradation. The essential steps involved are generally broken out into the sections that follow (Mills *et al.*, 1993):

$$\text{Semiconductor} + \text{photons (hv)} \rightarrow e^{-}(\text{CB}) + h^{+}(\text{VB}) \quad (1)$$

$$h^{+} + OH^{-} \rightarrow OH \quad (3)$$

$$e^{-} + O_2 \rightarrow O_2 \quad (4)$$

$$2e^{-} + O_2 + H_2O \rightarrow H_2O_2 \quad (5)$$

$$e^{-} + H_2O_2 \rightarrow OH + OH^{-} \quad (6)$$

Due to an excited electron and hole in the semiconductor, the dye is deteriorating. Many different semiconductors have been used, and the

bulk of them are used in the nano-state because of their improved surface area and positive impact on quantum size (Liu, 2012; Colmenares & Luque, 2014; Anpo *et al.*, 1987). As particle size decreases, QDs' increased surface area-to-volume ratio leads to a decrease in the recombination of the electron-hole pair. The photocatalytic activity of the smallest QDs is therefore expected to be higher than that of their bulk counterparts. This process facilitates the migration of holes and electrons to the QD's surface, where they can participate in the reaction. Figure 7 is representing the mechanism of photocatalytic action of degradation of dye.

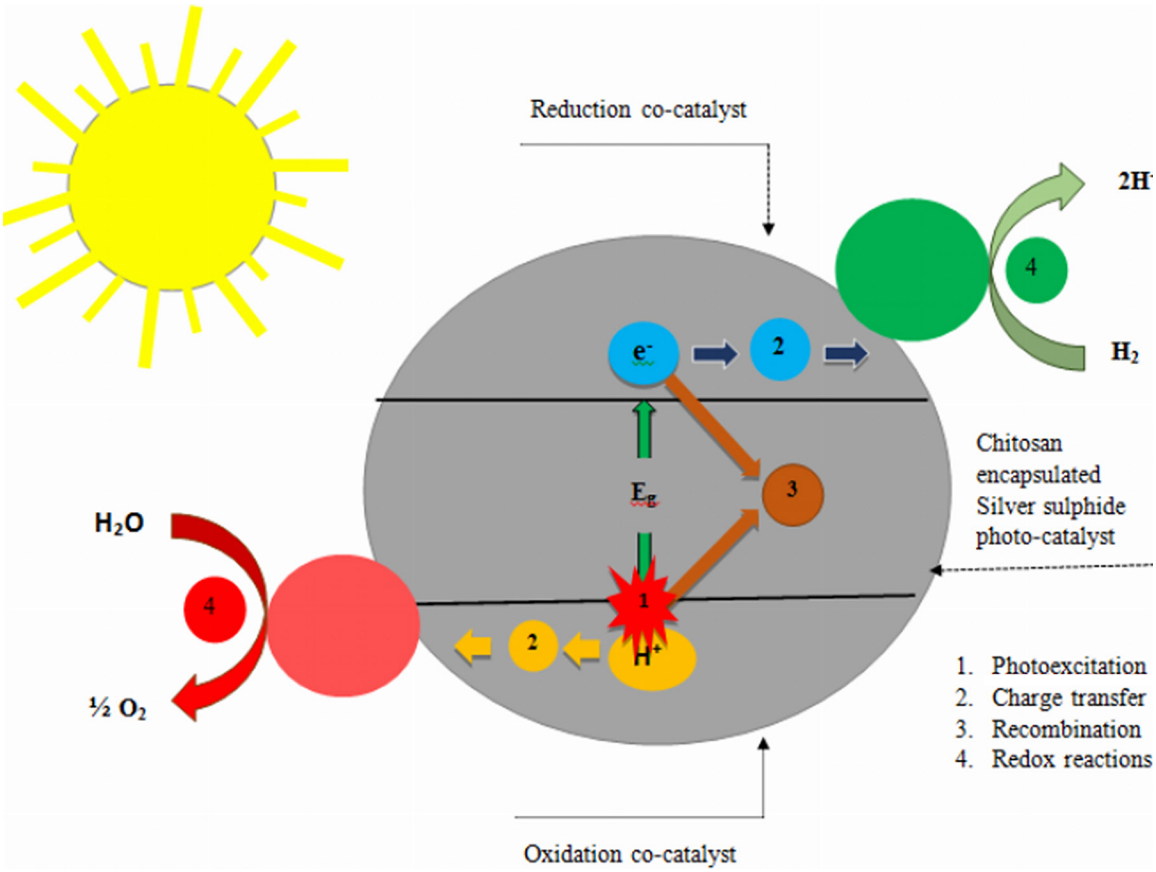

Figure 7. Representing the mechanism of photocatalytic action of degradation of dye. Modified form of Pant *et al.*, 2019.

5. CONCLUSION

In conclusion, this study successfully produced chitosan-encapsulated Ag_2S QDs with demonstrated effectiveness. The synthesis of these QDs was confirmed through XRD, HRTEM, FTIR, and EDX analyses. Notably, our photocatalytic results surpass those reported in the literature. XRD calculations revealed a crystallite size ranging from 8 to 12 nm for the synthesized samples. FTIR analysis identified several functional groups present in the QDs. Additionally, HRTEM determined the particle size to be 6 nm. Our experiment achieved remarkable degradation of 92% of ME dye within 1h, outperforming existing literature results. Notably, a pH of 9 enabled ~90% breakdown of ME, further highlighting the excellent performance of the synthesized samples in eliminating toxic dyes from the environment. Consequently, the chitosan-coated QDs hold significant promise as future photocatalytic agents.

Author contribution

All the authors contributed for shaping this research article.

Ethics declaration

The authors declare that they have no competing financial interests or personal relationships that could have appeared to influence the work reported in this research paper.

Acknowledgements

The authors are thankful to CPU Hamirpur for providing research facilities to complete this work as well as thankful for providing opportunity of presenting paper in international conference "Emerging Scenario of Science, Technology and Innovation-2023" (ESSTI-2023). The characterization was performed at "I.I.T Ropar" and "Saif lab of P.U. Chandigarh".

Conflicts of interest

There are no conflicts to declare. ♦

REFERENCES

Abdi-Ali, A., Hendiani, S., Mohammadi, P., & Gharavi, S. (2014). Assessment of biofilm formation and resistance to imipenem and ciprofloxacin among clinical isolates of Acinetobacterbaumannii in Tehran. Jundishapur. *Journal of Microbiology, 7(1).* https://doi.org/10.5812/jjm.8606

Alshehri, M. A., Aziz, A. T., Trivedi, S., & Panneerselvam, C. (2020). Efficacy of chitosan silver nanoparticles from shrimp-shell wastes against major mosquito vectors of public health importance. *Green Processing and Synthesis, 9(1),* 675-684.

Andrade, G. R., Nascimento, C. C., Neves, E. C., Santo Barbosa, C. D. A. E., Costa, L. P., Barreto, L. S., & Gimenez, I. F. (2012). One-step preparation of CdSnanocrystals supported on thiolated silica-gel matrix and evaluation of photocatalytic performance. *Journal of Hazardous Mmaterials*, 203, 151-157. https://doi.org/10.1016/j.jhazmat.2011.11.086

Anitha, R., Karthikeyan, B., Pandiyarajan, T., Vignesh, S., James, R. A., Vishwanathan, K., & Murari, B. M. (2011). Antifungal studies on biocompatible polymer encapsulated silver nanoparticles. *International Journal of Nanoscience, 10(04n05),* 1179-1183. https://doi.org/10.1142/S0219581X11008927

Anpo, M., Shima, T., Kodama, S., & Kubokawa, Y. (1987). Photocatalytic hydrogenation of propyne with water on small-particle titania: size quantization effects and reaction intermediates. *Journal of Physical Chemistry, 91(16),* 4305-4310. https://doi.org/10.1021/j100300a021

Anpo, M., Shima, T., Kodama, S., & Kubokawa, Y. (1987). Photocatalytic hydrogenation of propyne with water on small-particle titania: size quantization effects and reaction intermediates. *Journal of Physical Chemistry, 91(16),* 4305-4310. https://doi.org/10.1021/j100300a021

Coia, J. E., Duckworth, G. J., Edwards, D. I., Farrington, M., Fry, C., Humphreys, H., & Joint Working Party of the British Society of Antimicrobial Chemotherapy. (2006). Guidelines for the control and prevention of meticillin-resistant Staphylococcus aureus (MRSA) in healthcare facilities. *Journal of Hospital Infection, 63,* S1-S44. https://doi.org/10.1016/j.jhin.2006.01.001

Colmenares, J. C., & Luque, R. (2014). Heterogeneous photocatalyticnanomaterials: prospects and challenges in selective transformations of biomass-derived compounds. *Chemical Society Reviews, 43(3),* 765-778. https://doi.org/10.1039/C3CS60262A

Colmenares, J. C., & Luque, R. (2014). Heterogeneous photocatalyticnanomaterials: prospects and challenges in selective transformations of biomass-derived compounds. *Chemical Society Reviews, 43(3),* 765-778. https://doi.org/10.1039/C3CS60262A

Dodd, A. C., McKinley, A. J., Saunders, M., & Tsuzuki, T. (2006). Effect of particle size on the photocatalytic activity of nanoparticulate zinc oxide. *Journal of Nanoparticle Research, 8,* 43-51. https://doi.org/10.1007/s11051-005-5131-z

Durán, N., Marcato, P. D., Alves, O. L., De Souza, G. I., & Esposito, E. (2005). Mechanistic aspects of biosynthesis of silver nanoparticles by several Fusariumoxysporum strains. *Journal of Nanobiotechnology, 3,* 1-7. https://doi.org/10.1186/1477-3155-3-8

El-Khawaga, A. M., Farrag, A. A., Elsayed, M. A., El-Sayyad, G. S., & El-Batal, A. I. (2021). Antimicrobial and photocatalytic degradation activities of chitosan-coated magnetite nanocomposite. *Journal of Cluster Science, 32,* 1107-1119. https://doi.org/10.1007/s10876-020-01869-6

Govindan, S., Nivethaa, E. A. K., Saravanan, R., Narayanan, V., & Stephen, A. (2012). Synthesis and characterization of chitosan-silver

nanocomposite, Appl. https://doi.org/10.1007/s13204-012-0109-5

Habiba, K., Bracho-Rincon, D. P., Gonzalez-Feliciano, J. A., Villalobos-Santos, J. C., Makarov, V. I., Ortiz, D., … & Morell, G. (2015). Synergistic antibacterial activity of PEGylated silver-graphene quantum dots nanocomposites. Applied *Materials Today,1(2),* 80-87. https://doi.org/10.1016/j.apmt.2015.10.001

Huh, A. J., & Kwon, Y. J. (2011). "Nanoantibiotics": a new paradigm for treating infectious diseases using nanomaterials in the antibiotics resistant era. *Journal of Controlled Release*, *156(2),* 128-145. https://doi.org/10.1016/j.jconrel.2011.07.002

Iijima, M., & Kamiya, H. (2009). Surface modification for improving the stability of nanoparticles in liquid media. *KONA Powder and Particle Journal*, *27,* 119-129. https://doi.org/10.14356/kona.2009012

Jose, A., Devi, K. S., Pinheiro, D., & Narayana, S. L. (2018). Electrochemical synthesis, photodegradation and antibacterial properties of PEG capped zinc oxide nanoparticles. *Journal of Photochemistry and Photobiology B: Biology, 187,* 25-34. https://doi.org/10.1016/j.jphotobiol.2018.07.022

Li, Q., Mahendra, S., Lyon, D. Y., Brunet, L., Liga, M. V., Li, D., & Alvarez, P. J. (2008). Antimicrobial nanomaterials for water disinfection and microbial control: potential applications and implications. *Water Research, 42(18),* 4591-4602. https://doi.org/10.1016/j.watres.2008.08.015

Liu, S. Q. (2012). Magnetic semiconductor nano-photocatalysts for the degradation of organic pollutants. *Environmental Chemistry Letters, 10,* 209-216. https://doi.org/10.1007/s10311-011-0348-9

Ma, Q., Hu, X., Liu, N., Sharma, A., Zhang, C., Kawazoe, N., & Yang, Y. (2020). Polyethylene glycol (PEG)-modified $Ag/Ag_2O/Ag_3PO_4/Bi_2WO_6$ photocatalyst film with enhanced efficiency and stability under solar light. *Journal of colloid and Interface Science, 569,* 101-113. https://doi.org/10.1016/j.jcis.2020.02.064

Magesh, G., Bhoopathi, G., Nithya, N., Arun, A. P., & Ranjith Kumar, E. (2018). Effect of biopolymer blend matrix on structural, optical and biological properties of chitosan-agar blend ZnO nanocomposites. *Journal of Inorganic and Organometallic Polymers and Materials, 28,* 1528-1539. https://link.springer.com/article/10.1007/s10904-018-0848-1

Manikandan, A., & Sathiyabama, M. (2015). Green synthesis of copper-chitosan nanoparticles and study of its antibacterial activity. *Journal of Nanomedicine & Nanotechnology, 6(1),* 1. http://dx.doi.org/10.4172/2157-7439.1000251

Mills, A., Davies, R. H., & Worsley, D. (1993). Water purification by semiconductor photocatalysis. *Chemical Society Reviews, 22(6),* 417-425. https://doi.org/10.1039/CS9932200417

Muniz, F. T. L., Miranda, M. R., Morilla dos Santos, C., & Sasaki, J. M. (2016). The Scherrer equation and the dynamical theory of X-ray diffraction. ActaCrystallographica Section A: *Foundations and Advances, 72(3),* 385-390. https://doi.org/10.1107/S205327331600365X

Orooji, Y., Ghanbari, M., Amiri, O., & Salavati-Niasari, M. (2020). Facile fabrication of silver iodide/graphitic carbon nitride nanocomposites by notable Photocatalytic performance through sunlight and antimicrobial activity. *Journal of Hazardous Materials, 389,* 122079. https://doi.org/10.1016/j.jhazmat.2020.122079

Pant, B., Park, M., & Park, S. J. (2019). Recent advances in TiO2 films prepared by sol-gel methods for photocatalytic degradation of organic pollutants and antibacterial activities. *Coatings, 9(10),* 613. https://doi.org/10.3390/coatings9100613

Raghuram, H. S., Pradeep, S., Dash, S., Chowdhury, R., & Mazumder, S. (2016). Chitosan-encapsulated ZnS: M (M: Fe 3+ or Mn 2+) quantum dots for fluorescent labelling of sulphate-reducing bacteria. *Bulletin of Materials Science, 39,* 405-413. https://doi.org/10.1007/s12034-016-1178-y

Raza, Z. A., Khalil, S., Ayub, A., & Banat, I. M. (2020). Recent developments in chitosan encapsulation of various active ingredients for multifunctional applications. *Carbohydrate Research, 492,* 108004.https://doi.org/10.1016/j.carres.2020.108004

Sharma, A., Sharma, R., Bhatia, N., & Kumari, A. (2021). Review on synthesis, characterization and applications of silver sulphide quantum dots. *Journal of Materials Science Research and Reviews, 7(3),* 42-58. http://journal.pustakalibrary.com/id/eprint/166

Sharma, A., Sharma, R., Thakur, N., Sharma, P., & Kumari, A. (2023). Silver sulphide (Ag_2S) quantum dots synthesized from aqueous route with enhanced antimicrobial and dye degradation capabilities. *Physica E: Low-dimensional Systems and Nanostructures,* 115730. https://doi.org/10.1016/j.physe.2023.115730

Tan, L., Wan, A., & Li, H. (2013). Ag_2S quantum dots conjugated chitosan nanospheres toward light-triggered nitric oxide release and near-infrared fluorescence imaging. *Langmuir, 29(48),* 15032-15042 (dx.doi.org/10.1021/la403028j. http://dx.doi.org/10.1021/la403028j

Zhang, G., Li, J., Shen, A., & Hu, J. (2015). Synthesis of size-tunable chitosan encapsulated gold-silver nanoflowers and their application in SERS imaging of living cells. *Physical Chemistry Chemical Physics, 17(33),* 21261-21267. https://doi.org/10.1039/C4CP05343E

Kusiak-Nejman, E., Sienkiewicz, A., Wanag, A., Rokicka-Konieczna, P., & Morawski, A. W. (2021). The role of adsorption in the photocatalytic decomposition of dyes on APTES-Modified TiO_2 nanomaterials. *Catalysts, 11(2),* 172. https://doi.org/10.3390/catal11020172

Dutta, V., Sudhaik, A., Raizada, P., Singh, A., Ahamad, T., Thakur, S., & Singh, P. (2023). Tailoring S-scheme-based carbon nanotubes (CNTs) mediated Ag-$CuBi_2O_4/B_{i2}S_3$ nanomaterials for photocatalytic dyes degradation in the aqueous system. *Journal of Materials Science & Technology.* https://doi.org/10.1016/j.jmst.2023.03.037

Sudhaik, A., Raizada, P., Ahamad, T., Alshehri, S. M., Nguyen, V. H., Van Le, Q., & Singh, P. (2022). Recent advances in cellulose supported photocatalysis for pollutant mitigation: A review. *International Journal of Biological Macromolecules*. https://doi.org/10.1016/j.ijbiomac.2022.11.241

Hasija, V., Raizada, P., Sudhaik, A., Sharma, K., Kumar, A., Singh, P., & Thakur, V. K. (2019). Recent advances in noble metal free doped graphitic carbon nitride based nanohybrids for photocatalysis of organic contaminants in water: a review. *Applied Materials Today, 15,* 494-524. https://doi.org/10.1016/j.apmt.2019.04.003

Kumar, Y., Kumar, R., Raizada, P., Khan, A. A. P., Van Le, Q., Singh, P., & Nguyen, V. H. (2021). Novel Z-Scheme ZnIn2S4-based photocatalysts for solar-driven environmental and energy applications: Progress and perspectives. *Journal of Materials Science & Technology, 87.* https://doi.org/10.1016/j.jmst.2021.01.051

Sudhaik, A., Raizada, P., Khan, A. A. P., Singh, A., & Singh, P. (2022). Graphitic carbon nitride-based upconversionphotocatalyst for hydrogen production and water purification. *Nanofabrication, 7,* 280-313. https://doi.org/10.37819/nanofab.007.189

Barragan, J. A., Aleman Castro, J. R., Peregrina-Lucano, A. A., Sánchez-Amaya, M., Rivero, E. P., & Larios-Durán, E. R. (2021). Leaching of metals from e-waste: from its thermodynamic analysis and design to its implementation and optimization. *ACS Omega, 6(18),* 12063-12071. https://doi.org/10.1021/acsomega.1c00724

Abd Elkodous, M., El-Sayyad, G. S., Youssry, S. M., Nada, H. G., Gobara, M., Elsayed, M. A., … & Matsuda, A. (2020). Carbon-dot-loaded $CoxNi1^{-}$ xFe_2O_4; x= $0.9/SiO_2/TiO_2$ nanocomposite with enhanced photocatalytic and antimicrobial potential: An engineered nanocomposite for wastewater treatment. *Scientific Reports, 10(1),* 11534. http://doi.org/10.1038/s41598-020-68173-1

Vasiljevic, Z. Z., Dojcinovic, M. P., Vujancevic, J. D., Jankovic-Castvan, I., Ognjanovic, M., Tadic, N. B., Stojadinovic, S., Brankovic, G. O. and Nikolic, M. V., 2020. Photocatalytic degradation of methylene blue under natural sunlight using iron titanate nanoparticles prepared by a modified sol-gel method. *Royal Society Open Science, 7(9),* p.200708. https://doi.org/10.1098/rsos.200708